Nip1p Associates with 40 S Ribosomes and the Prt1p Subunit of Eukaryotic Initiation Factor 3 and Is Required for Efficient Translation Initiation*

(Received for publication, April 23, 1998, and in revised form, June 25, 1998)

Jay R. Greenberg‡, Lon Phan§¶, Zhenyu Gu‡‖, Aravinda deSilva‡ **, Christopher Apolito‡, Fred Sherman‡‡, Alan G. Hinnebusch§, and David S. Goldfarb‡ §§

From the ‡Department of Biology, University of Rochester, Rochester, New York 14627, the §Laboratory of Eukaryotic Gene Regulation, NICHD, National Institutes of Health, Bethesda, Maryland 20892, and the ‡‡Department of Biochemistry and Biophysics, University of Rochester Medical School, Rochester, New York 14642

Nip1p is an essential *Saccharomyces cerevisiae* protein that was identified in a screen for temperature conditional (ts) mutants exhibiting defects in nuclear transport. New results indicate that Nip1p has a primary role in translation initiation. Polysome profiles indicate that cells depleted of Nip1p and *nip1-1* cells are defective in translation initiation, a conclusion that is supported by a reduced rate of protein synthesis in Nip1p-depleted cells. Nip1p cosediments with free 40 S ribosomal subunits and polysomal preinitiation complexes, but not with free or elongating 80 S ribosomes or 60 S subunits. Nip1p can be isolated in an about 670-kDa complex containing polyhistidine-tagged Prt1p, a subunit of translation initiation factor 3, by binding to Ni^{2+}-NTA-agarose beads in a manner completely dependent on the tagged form of Prt1p. The *nip1-1* ts growth defect was suppressed by the deletion of the ribosomal protein, *RPL46*. Also, *nip1-1* mutant cells are hypersensitive to paromomycin. These results suggest that Nip1p is a subunit of eukaryotic initiation factor 3 required for efficient translation initiation.

Translation initiation can be considered to begin with the dissociation of 80 S ribosomes into free 40 S and 60 S subunits which then reassociate with mRNAs in a highly regulated and complex process. Initiation of cap-dependent translation in eukaryotes begins with the binding of a 43 S preinitiation complex to the 5′ cap of the mRNA. The 43 S ribosome migrates down the mRNA to the translation start site where it is joined by a 60 S ribosomal subunit to complete the assembly of an apparatus capable of accurately forming the first peptide bond. Translation initiation is mediated by at least 10 translation initiation factors, many of which contain multiple subunits that are conserved between yeast and mammals (reviewed in Refs. 1). eIF3[1] is the most complex initiation factor and the one which is least understood with regard to both composition and function. Human eIF3, which is composed of at least nine distinct subunits (2–5), stimulates multiple steps of translation initiation, including the dissociation of 80 S ribosomes, stabilizing $tRNA_i^{Met}$ binding to 40 S ribosomal subunits, and binding of mRNA to 40 S subunits (1). A yeast eIF3 complex was purified on the basis of replacing mammalian eIF3 in an *in vitro* translation initiation assay (6). This complex contains eight subunits of masses 16, 21, 29, 33, 39, 62, 90, and 135 kDa. The 16-, 39-, 62-, and 90-kDa subunits were identified as Sui1p (7, 8), Tif34p (9) Gcd10p (10), and Prt1p (11), respectively. Yeast Prt1p is 36% identical to the 116-kDa subunit of human eIF3, and Tif34p, a WD repeat protein, is 46% identical to the p36 subunit of human eIF3. Tif34p is required for cell cycle progression and mating as well as translation initiation (12). However, Gcd10p and Sui1p do not show strong similarities to any human eIF3 subunits (13). p33 was shown to interact with Tif34p and Prt1p by two-hybrid analysis and co-immunoprecipitation. It has a RNA-binding domain which does not seem to be essential for function (12).

Sui1p is an essential protein identified genetically by its role in ribosomal recognition of the AUG start codon during scanning (7) and is 57% identical in amino acid sequence to rabbit eIF1 (14). Gcd10p is an essential RNA-binding protein first identified by its involvement in regulating translation initiation on *GCN4* mRNA. Because *GCN4* translation is coupled to the availability and utilization of the ternary complex containing eIF2, GTP, and $tRNA_i^{Met}$ (15), these genetic findings implicated Gcd10p in the binding of ternary complexes to 40 S ribosomal subunits (10). Human eIF3 contains a 66-kDa RNA-binding subunit that shares an epitope with Gcd10p (10); however, human p66 shows little primary sequence similarity to yeast Gcd10p (13).

It was recently reported by Asano *et al.* (2) that the p110 subunit of human eIF3 is 31% identical to yeast Nip1p; however, Nip1p was not detected in their yeast eIF3 preparation. A different complex containing Prt1p was purified using reactivity against Prt1p antibodies as the means of detecting the protein (16). This complex was shown to restore translation in a cell-free extract derived from a temperature-sensitive *prt1-1* mutant. Interestingly, the complex contained a polypeptide of an apparent mass similar to Nip1p. We now show that Nip1p indeed co-purifies with Prt1p.

* This work was supported in part by the American Cancer Society Grant BE-104B (to D. S. G.) and National Institutes of Health Research Grant R01 GM12702 (to F. S.). The costs of publication of this article were defrayed in part by the payment of page charges. This article must therefore be hereby marked "*advertisement*" in accordance with 18 U.S.C. Section 1734 solely to indicate this fact.

¶ Supported by a National Research Council post-doctoral fellowship.

‖ Present address: Cardiovascular Research Center, Dept. of Medicine, Harvard Medical School, MGH East, Charlestown, MA 02129.

** Present address: Dept. of Epidemiology & Public Health, Yale University School of Medicine, 60 College St., P. O. Box 208034, New Haven, CT 06520-8034.

§§ To whom correspondence should be addressed: Dept. of Biology, University of Rochester, Rochester, NY 14627. Tel.: 716-275-3890; Fax: 716-275-2070; E-mail: dasg@uhura.cc.rochester.edu.

[1] The abbreviations used are: eIF3, eukaryotic initiation factor 3; kb, kilobase pair(s); PCR, polymerase chain reaction; FOA, 5-fluoroorotic acid; PAGE, polyacrylamide gel electrophoresis; RSW, ribosomal salt wash.

TABLE I
Yeast strains

Strain	Genotype	Source
B-8106	*MAT**a** cyc1-NLS cyc7–67 ura3–52 lys5–10*	Ref. 17
B-8302	*MAT**a** cyc1-NLS cyc7–67 ura3–52 lys5–10 nip1–1*	Ref. 17
B-8305	B-8302 *p[NIP1-HA]*	Ref. 17
DG-11	*MATα CYC1 cyc7–67 his3-Δ1*	This study
DG-453	*MAT**a** cyc1-NLS cyc7–67 ura3–52 his3-Δ1 nip1–1*	This study
DG-137	*MAT**a** cyc1-NLS cyc7–67 ura3–52 his3-Δ1 nip1–1 snp1–1*	This study
DG-448	*MAT**a** cyc1-NLS cyc7–67 ura3–52 lys5–10 nip1–1 rpl46-Δ*	This study
DG-130	*MAT**a** cycl-NLS cyc7–67 ura3–52 lys5–10 nip7–1*	This study
Ad	*MAT**a** ade2 his3 leu2 trp1 ura3 can1 [ρ+ L-0 M-0]*	P. Sarnow
DG-449	*MAT**a** ade2 his3 leu2 trp1 ura3 can1 [ρ+ L-0 M-0]* pNIP1*[NIP1 URA3]*	This study
DG-450	*MAT**a** ade2 his3 leu2 trp1 ura3 can1 nip1::kan*^{1} · *[ρ+ L-0 M-0]* pNIP1*[NIP1 URA3]*	This study
DG-451	*MAT**a** ade2 his3 leu2 trp1 ura3 can1 nip1::kan*^{1} · *[ρ+ L-0 M-0]* pNIP1*[NIP1 URA3]*pUBI-R-NIP1*[UBI1::NIP1 LEU2]*	This study
DG-452	*MAT**a** ade2 his3 leu2 trp1 ura3 can1 nip1::kan*^{1} · *[ρ+ L-0 M-0]* pUBI-R-NIP1 *[UBI1::NIP1 LEU2]*	This study
DG-454	*MAT**a** ade2 his3 leu2 trp1 ura3 can1 nip1::kan*^{1} · *[ρ+ L-0 M-0]* pNIP1*[NIP1 URA3]pUBI-M-NIP1 [UBI1::NIP1 LEU2]*	This study
DG-455	*MAT**a** ade2 his3 leu2 trp1 ura3 can1 nip1::kan*^{1} · *[ρ+ L-0 M-0]* pUBI-M-NIP1*[UBI1::NIP1 LEU2]*	This study
TB11B-4–1	*MAT**a** prt1–1 leu2–3 leu2–112 ura3–52 ade1*	G. Johnston
H1676	*MAT**a** prt1–1 leu2–3 leu2–112*	This study
LPY100	*MAT**a** prt1–1 leu2–3 leu2–112* pJA100*[PRT1 URA3]*	This study
LPY101	*MAT**a** prt1–1 leu2–3 leu2–112* pLP101*[PRT1-His URA3]*	This study
LPY199	*MAT**a** leu2–3 leu2–112 prt1-KanMX* pLP102*[PRT1 LEU2]*	This study
LPY200	*MAT**a** leu2–3 leu2–112 prt1-KanMX* pLP100*[PRT1-SalI URA3]*	This study
LPY201	*MAT**a** leu2–3 leu2–112 prt1-KanMX* pLP101*[PRT1-His URA3]*	This study

NIP1 encodes an essential 93-kDa protein that localizes predominantly to the cytoplasm (17). The *nip1-1* allele was identified in a screen for mutants with defects in nuclear transport, and *nip1-1* ts cells were defective in nuclear localization signal-directed nuclear transport (17). Analysis of *nip1-1* ts cells using a recently developed assay based on the nuclear import kinetics of nuclear localization signal-containing green fluorescent protein confirmed that the transport defect is temperature conditional (18). Here, we show that Nip1p is likely to play an essential role in protein synthesis as a subunit of yeast eIF3.

MATERIALS AND METHODS

Yeast Strains, Plasmids, and Growth Conditions—The major yeast strains used in this study are listed in Table I. The major plasmids used are YCp50, a centromere-carrying (CEN) shuttle vector (19); pSNP1, constructed by insertion of a 2.5-kb *Kpn*I fragment encompassing the *SNP1/RPL46* gene at the *Kpn*I site of YCplac33 (20); pNIP1 which has a wild-type *NIP1* gene inserted into YCp50 at the *Hin*dIII site (17); pAS195 (obtained from A. Sachs), containing a *rpl46-Δ::URA3* construct; pUBI-R-NIP1 containing a ubiquitin-*NIP1* fusion gene in which the *NIP1* coding sequence starts with an arginine codon; pJA100 containing wild-type *PRT1;* pLP101 containing histidine-tagged *PRT1* (*PRT1-His*). Previously described methods and media were used for testing and genetic analysis of general yeast mutations (21, 22). Standard YPD medium, denoted glucose medium in this paper, and synthetic media used for growing and testing yeast strains have been described by Sherman (22).

Construction of pUBI-R-NIP1—The *GAL10* promoter and ubiquitin coding sequence were obtained from pUB23 (23). The plasmid was digested with *Acc*I and blunt ended with mung bean nuclease. It was then digested with *Bam*HI. A *NIP1* PCR product was prepared which included all of the *NIP1* coding sequence except the initial AUG and also had 300 nucleotides downstream from the termination codon. It had a *Bam*HI site at the 5′ end and a *Hin*dIII site at the 3′ end. The two primers used were: TACGGGATCCTCCCGTTTCTTTTCGTCTAA (N-terminal) and ATATCATACTAAGCTTAAAGTTTAATAGTTTGTATT (C-terminal). The template used was pNIP1. The resulting PCR product, which had a size of 2.45 kb, was digested with *Bam*HI and *Hin*dIII. The yeast *CEN* shuttle vector YCplac111 (20) which has a *LEU2* selectable marker was digested with *Sma*I and *Hin*dIII. The large fragment from this digest was then ligated together with the fragment from pUB23 and the *NIP1* PCR product.

Construction of pJA100 and pLP101—A *Cla*I DNA fragment containing *PRT1* was ligated to plasmid pRS316 (24), yielding plasmid pJA100. To construct plasmid pLP102, *PRT1* was excised from pJA100 by digesting with *Cla*I and *Pst*I and ligated to pRS315 (24). Plasmid pLP101, encoding the Prt1p protein tagged with eight histidines at its C terminus, was constructed in the following two steps. The method of PCR fusion (25) was used to mutate nucleotide 2172 of *PRT1*, numbered relative to the translation start site, from A to C, resulting in the creation of *PRT1-SalI* that contains the newly formed *Sal*I restriction site immediately prior to the stop codon. This mutation changes the last amino acid of Prt1p from a glutamic acid to an aspartic acid residue. Two mutagenic 72-mer oligonucleotides, used to generate the mutation, were complementary from nucleotides 2136–2208. Two flanking 20-mer oligonucleotides used for making the PCR fusion product started from nucleotide 1618 and 2497, respectively. The final 879-base pair PCR fusion product and plasmid pJA100 were digested with *Bam*HI plus *Pst*I and ligated together to form plasmid pLP100. Two complementary oligonucleotides were annealed to form a DNA duplex containing eight consecutive histidine codons and *Sal*I sites at each end. The ends of the duplex were phosphorylated with T4 kinase and ligated to plasmid pLP100 that had been digested with *Sal*I and dephosphorylated with calf intestine phosphatase, producing pLP101. Henceforth, the allele on pLP101 will be referred to as *PRT1-His*.

Construction of nip1-Δ Strain Bearing a Plasmid Copy of the Ubiquitin-NIP1 Fusion Gene—The strain Ad which is a W303-1A derivative cured of double-stranded RNA killer particles (26) was utilized. It was first transformed with the *URA3* plasmid pNIP1 to give DG-449. The chromosomal *NIP1* gene was disrupted by the *kan*^{r} gene encoding kanamycin resistance by means of PCR-based gene disruption (27). The primers consisted of oligonucleotides having 45 bases corresponding to sequences at the beginning or end of the *NIP1* coding sequence and 19 bases complementary to sequences in the plasmid pUG6 which was used as the template. Strain DG-449 was transformed with the *kan*^{r} PCR product by the lithium acetate procedure (28). Kanamycin-resistant transformants were selected on YPD plates containing 200 μg/ml G418 (Life Technologies, Inc.). Transformants in which the chromosomal copy of the *NIP1* gene was disrupted were selected on the basis of their inability to grow on SC medium containing 5-fluoroorotic acid (FOA, 1 μg/ml) because they require a plasmid copy of the *NIP1* gene. Cells which have a functional *URA3* gene are unable to grow on FOA medium (29). The presence of a *NIP1* gene disrupted by the *kan*^{r} gene was verified by PCR with appropriate primers. A *nip1-Δ* clone designated DG-450 was transformed with the plasmid pUBI-R-NIP1, and transformants were selected on SC medium lacking leucine. After streaking one of these transformants onto YPG medium which contained 2% galactose instead of glucose, a transformant, DG-452, lacking pNIP1 was selected by growth on SC medium containing FOA and 2% galactose.

Construction of prt1-Δ Strains Bearing Plasmid-borne PRT1 or PRT1-His Alleles—The *prt1-1* strain H1676 was constructed by tetrad analysis of a cross involving strain TP11B-4-1 (provided by G. Johnston) and was transformed with plasmid pJA100 or pLP101 to yield strains LPY100 and LPY101, respectively. PCR-based gene disruption (30) was used to replace chromosomal *PRT1* in LPY101 with the *kanMX* module encoding kanamycin resistance. Plasmid pFA6 (30) was used as the template for amplifying the KanMX module by PCR using oligonucleo-

tides containing 19–22 nucleotides corresponding to the multiple cloning sequences flanking the module and 35 nucleotides corresponding to sequences either immediately upstream of the start codon or downstream of the stop codon of *PRT1*. The 1.3-kb PCR product was used to transform LPY101 by the lithium acetate method (31), resulting in growth on YPD plates containing 200 μg/ml G418 (Life Technologies, Inc.). The G418^r (resistant) clones were screened for disruption of the chromosomal *PRT1* gene by determining their viability with and without plasmid pLP101 containing *PRT1*. This was accomplished by testing the transformants on SC plates supplemented with 5-FOA (1 μg/ml) (29) on which Ura$^+$ cells unable to lose plasmid pLP101 could not grow. To eliminate false positives, we showed that the G418^r 5-FOA^s (sensitive) strains thus identified could be cured of plasmid pLP101 on medium containing 5-FOA after introduction of the *LEU2* plasmid pLP102 bearing *PRT1*. One such Ura$^-$ Leu$^+$ strain, LPY199, was used for producing isogenic strains LPY200 and LPY201 which contained the *PRT1-SalI* gene in the pLP100 plasmid or the *PRT1-His* gene in the plasmid pLP101, respectively. Following introduction of pLP100 or pLP101, the resulting Ura$^+$ Leu$^+$ transformants were cultured on minimal medium supplemented with leucine to allow loss of the *LEU2 PRT1* plasmid pLP102.

Cloning and Sequencing of the SNP1/RPL46 Gene—The *SNP1/RPL46* gene was cloned by first complementing the *ura3-52* marker in the *nip1-1 snp1-1* strain DG-102 with a YCp50 genomic bank (19). The Ura$^+$ transformants were suspended and streaked on glucose plates, which were incubated at 18 °C. Plasmids complementing *snp1-1* in the presumptive *SNP1*$^+$ transformants were transferred from yeast to *Escherichia coli* and analyzed with restriction endonucleases. After examining a number of plasmids with various deletions, the 2.5-kb *Kpn*I restriction fragment was transferred to the plasmid YCplac33 (20) and was shown to complement the *snp1-1* growth defect.

Double-strand DNA of *SNP1* was sequenced with Sequenase as described by manufacturer (U.S. Biochemical Corp.). Sequences were analyzed with the University of Wisconsin Genetics Computer Group programs (32).

Disruption of RPL46—One-step gene disruption was used to delete the chromosomal *RPL46* gene. The plasmid pAS195 contains a *RPL46* disrupted with the selectable marker *URA3* (*rpl46-Δ::URA3*). B-8302 (*nip1-1*) was transformed with a linear restriction fragment containing *rpl46-Δ::URA3*. Stable Ura$^+$ transformants were selected and tested for cold-sensitive growth at 18 °C.

Antibiotic Sensitivity Assay—Resistance and sensitivity to paromomycin and cycloheximide were scored by spotting cells grown to exponential phase on YPD or synthetic media containing various concentrations of the antibiotics and examining the plates after incubation at 30 °C for 6 days.

Protein Synthesis—[^{35}S]Methionine and [^{35}S]cysteine incorporation into hot trichloroacetic acid-insoluble material were measured as follows: DG-452 cells and Ad wild-type cells were grown at 30 °C to early log phase in SC medium containing 0.5% galactose plus 1.5% raffinose but lacking methionine. After shifting to medium containing 2% glucose by spinning down and resuspending, the absorbance at 600 nm was read, then each 4.5-ml culture was mixed with 5 μCi of ^{35}S-protein labeling mixture (1175 Ci/mmol, NEN Life Technologies Inc.). At 10-min intervals, 0.5-ml aliquots were mixed with 0.5 ml of 25% trichloroacetic acid. When all samples had been collected, they were heated at 95 °C for 10 min. Precipitated proteins were collected on glass microfiber filter discs (Gelman type AE), washed first with 5% trichloroacetic acid and then with 95% ethanol. ^{35}S incorporation was quantified by liquid scintillation counting. Protein synthesis rates (cpm/min/A_{600}) were calculated by fitting curves to the incorporation data with the aid of a computer. During incubation in glucose medium, the absorbance at 600 nm of the cultures were kept between 0.1 and 0.3 by diluting with fresh medium as necessary.

Preparation of Anti-Nip1p Polyclonal Antibodies—A *Sal*I-*Hin*dIII restriction fragment coding for the C-terminal 334 amino acids of Nip1p was inserted into the bacterial expression vector, pTrcHisA (Invitrogen, San Diego, CA). After isopropyl-1-thio-β-D-galactopyranoside induction in *E. coli*, the fusion protein was isolated as an inclusion body, then purified by excision from preparative SDS-PAGE gels. Polyclonal antibodies were commercially prepared by BabCo (Berkeley, CA) and affinity purified by binding to the bacterially expressed fusion protein immobilized on a nitrocellulose membrane.

Sucrose Gradient Analysis of Ribosomes—Yeast cells were grown to early log phase in YP (A_{600} = 0.4–0.8) or synthetic media (A_{600} = 0.4–0.6), treated with 100 μg/ml cycloheximide for 10 min, harvested by centrifugation, and lysed by vortexing with glass beads in breaking buffer (20 mM HEPES-KOH, pH 7.4, 2 mM magnesium acetate, 0.1 M KCl, 15 mM β-mercaptoethanol, and 100 μg/ml cycloheximide). The crude cell extract was centrifuged at 8,000 rpm in a Sorvall SS34 rotor for 5 min at 4 °C. Ten to 20 A_{254} units of the supernatant were loaded onto 10-ml sucrose gradients containing 10 mM Tris-HCl, pH 7.4, 70 mM ammonium acetate, 4 mM magnesium acetate. The gradients were centrifuged at 40,000 rpm, 4 °C in a Beckman SW 41 rotor for 2.5, 4, or 7.5 h as indicated, then scanned at 254 nm with an ISCO UA-5 absorbance monitor.

Immunoblotting—To assay for the presence of Nip1p, proteins in sucrose gradient fractions were precipitated by 10% trichloroacetic acid and washed with acetone or ethanol. The pellets were resuspended in protein gel loading buffer, separated on 10% SDS-polyacrylamide gels, and transferred electrophoretically to polyvinylidene difluoride or nitrocellulose filters, which were then blocked with isotonic buffered saline containing 2–3% nonfat dry milk and, in some cases, 0.5% Tween 20 (polyvinylidene difluoride membranes only). After incubation at room temperature with anti-Nip1 polyclonal antibody or with anti-HA monoclonal antibody 12CA5 (BAbCo, Richmond, CA), the filters were washed and incubated with alkaline phosphatase-conjugated secondary antibodies (Bio-Rad). After washing again, antibody binding was detected by staining with nitro blue tetrazolium and 5-bromo-4-chloro-3-indolyl phosphate. To assess the content of Nip1p in whole cell extracts during Nip1p depletion experiments, extracts were prepared from cells grown in galactose medium, then incubated in glucose medium for the indicated times. Extracts were made as for sucrose gradient analysis of ribosomes except that a protease inhibitor mixture was added to the cell pellets before breaking the cells (Sigma catalog number P-8215). 50 μl were used per gram of packed cells.

Preparation of Ribosomal Salt Wash (RSW)—RSW fractions were prepared essentially as described previously (16) with minor modifications. Strains LPY200 and LPY201 were grown in 6 liters of YPD medium to an A_{600} of 7.5–8.0, harvested by centrifugation at 7,000 × *g* for 15 min, and washed with ice-cold water. All subsequent steps were performed at 4 °C. About 60 g of cells were resuspended in 120 ml of Buffer A (20 mM Tris-HCl, pH 7.5, 100 mM KCl, 5 mM $MgCl_2$, 0.1 mM EDTA, 7 mM β-mercaptoethanol, 1 mM phenylmethylsulfonyl fluoride, 1 × Complete^{TM} protease inhibitor mixture (Boehringer Mannheim)) and homogenized in a bead beater with 2 cell volumes of glass beads. The cells were homogenized eight times for 30 s and cooled on ice for 30 s between cycles. The pooled homogenate was clarified by centrifugation at 17,000 × *g* and then at 25,000 × *g* for 15 min, and ribosomes were subsequently pelleted at 200,000 × *g* for 2 h. The ribosomal pellet was resuspended in 25 ml of Buffer B (Buffer A containing 350 mM KCl) and centrifuged at 200,000 × *g* for 2 h. The supernatant containing the RSW fraction was dialyzed against 1 liter of binding buffer (20 mM Tris-HCl, pH 7.5, 350 mM KCl, 5 mM $MgCl_2$, 7 mM β-mercaptoethanol, 10% glycerol, 1 mM phenylmethylsulfonyl fluoride, and 20 mM imidazole) for 1 h.

Ni^{2+}-NTA-Agarose Chromatography—Whole cell extract or dialyzed RSW fraction was bound to Ni^{2+}-NTA-agarose (Qiagen) in batch format using 0.2 ml of a 50% suspension of resin in binding buffer per liter of starting cell culture. The mixture was placed in a 15-ml conical tube and rocked for 1.5 h at 4 °C. The Ni^{2+}-NTA-agarose resin was pelleted at 1,000 × *g* for 5 min, washed with 10 ml of binding buffer three times, resuspended in 3 ml of elution buffer (binding buffer containing 60 mM imidazole), and packed by gravity into a 2-ml column (Bio-Rad). Fractions were collected and analyzed by SDS-PAGE and immunoblot analysis using antibodies against Prt1p (33) or against Nip1p.

Sepharose-6 FPLC—Total yeast extract was prepared from 60 g of strain LPY100 or LPY101 in breaking buffer (20 mM Tris-HCl, pH 7.5, 100 mM KCl, 5 mM $MgCl_2$, 7 mM β-mercaptoethanol, 20 mM imidazole, 1 mM phenylmethylsulfonyl fluoride, and 1 × Complete^{TM} protease inhibitor mixture) and clarified by centrifugation first at 17,000 × *g* and then at 25,000 × *g* for 15 min, as above. The supernatant was bound immediately to Ni^{2+}-NTA-agarose and the resin was washed with breaking buffer and eluted with breaking buffer containing 60 mM imidazole. The fractions containing Prt1p-His, as determined by immunoblot analysis, were pooled, dialyzed against GF buffer (50 mM sodium phosphate buffer, pH 7.0, and 150 mM NaCl), and concentrated using a Centricon-10 spin column (Amicon) to a volume of 300 μl and a final protein concentration of 1–1.5 μg/μl. An aliquot (200 μl) of the concentrated eluate was injected onto a Sepharose-6 sizing column of a fast phase liquid chromatography system (Pharmacia Biotech) and chromatographed in GF buffer at a flow rate of 0.4 ml/min, collecting 0.4-ml fractions. This column separates proteins in the molecular mass range of 5 × 10^3 to 1 × 10^6 kDa. Fractions were analyzed by SDS-PAGE followed by silver staining using the SilverXpress^{TM} kit purchased from Novex or by immunoblot analysis as described above.

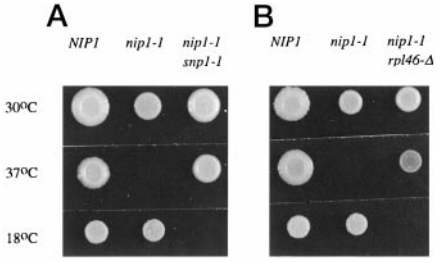

FIG. 1. **Mutations in 60 S subunit protein L46 suppress the *nip1-1* growth defect.** *A,* growth of *NIP1*$^+$ (DG-11), *nip1-1* (DG-453), and *nip1-1 snp1-1* (DG-137), and *B, NIP1*$^+$ (B-8106), *nip1-1* (B-8302), *nip1-1 rpl46-*Δ (DG-448) at 18, 30, and 37 °C for 4 days on YPD plates.

RESULTS

Mutations in Ribosomal Protein L46 Suppress the nip1-1 Growth Defect—To identify possible interacting partners for Nip1p, we isolated extragenic mutations that suppressed the *nip1-1* growth defect at 37 °C. *Suppressors* of *nip1-1* (*snp*) were isolated from UV mutagenized cells that grew better than the *nip1-1* strain B-8302 at 37 °C. One of these, *snp1-1*, was cold-sensitive for growth at 18 °C (Fig. 1*A*). The *SNP1* gene was cloned from a YCp50 genomic bank (19) by complementing the cold-sensitive growth defect of the *snp1-1 nip1–1* strain (DG-137). *SNP1* was identified as *RPL*46 by deletion mapping. This gene encodes the 60 S ribosomal subunit protein L46 (34). Although we did not determine the nature of the *snp1-1* mutation, the total loss of *RPL46* function has been reported to cause cold sensitivity in some strains (35).

To investigate whether loss of *RPL46* function could suppress the *nip1-1* temperature-sensitive growth defect, the chromosomal *RPL46* gene was disrupted in strain B-8302 (*nip1-1*) with a *rpl46-*Δ*::URA3* restriction fragment from the plasmid pAS195 (provided by A. Sachs). *rpl46-*Δ *nip1-1* cells (DG-448) grew moderately well at 37 °C but were cold-sensitive for growth at 18 °C (Fig. 1*B*). Therefore, the deletion of *RPL46* suppresses the *nip1-1* ts defect. Mutation of *RPL46* has been previously shown to suppress mutations in *PAB1* (36), which encodes the cytoplasmic poly(A)-binding protein known to function in translation initiation, and *SIS1*, which encodes a 40 S ribosome-associated DnaJ homologue also having a putative role in translation initiation (37). This result suggested that Nip1p may play a role in protein synthesis.

The nature of the *nip1-1* mutation was determined by sequencing multiple PCR fragments to be a point mutation (T to A) at position 900 relative to the translation start site. This change resulted in amino acid 300 being changed from isoleucine to asparagine. The mutation was verified by resequencing the corresponding region of the wild-type gene.

nip1-1 Cells Are Hypersensitive to Paromomycin—Nip1p contains a serine-rich acidic domain that is similar to an extended motif in Nsr1p, a nucleolar protein that, like Nip1p, was initially associated with nuclear transport (38, 39). Because mutations in *NSR1* were shown to cause hypersensitivity to paromomycin, an inhibitor of protein synthesis, we examined *nip1-1* cells for paromomycin sensitivity. Paromomycin and similar aminoglycoside antibiotics increase codon misreading in bacteria and eukaryotes (40, 41). B-8106 (*NIP1*$^+$) grew normally when spread on YPD plates containing 2.5 mg/ml paromomycin, whereas B-8302 (*nip1-1*) did not grow (data not shown). Two different *nip1-1* strains (B-8302 and DG-453) responded similarly to these drug tests, indicating that the drug phenotypes are independent of genetic background. When a wild-type *NIP1* gene on a CEN plasmid was introduced into the *nip1-1* mutant strain B-8302, its sensitivity to drugs reverted to that of the isogenic *NIP1*$^+$ strain (B-8106).

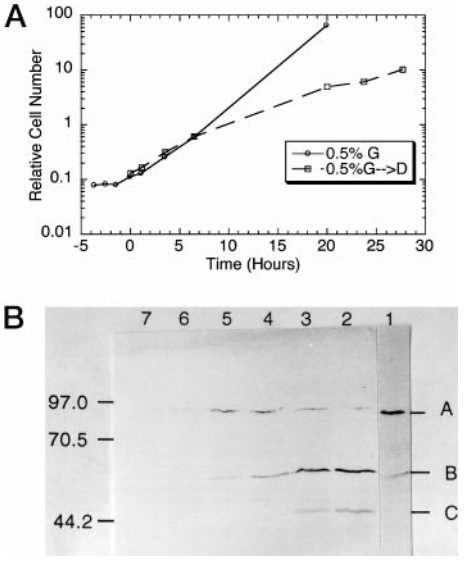

FIG. 2. **DG-452 cells incubated in glucose medium have a reduced growth rate and a reduced content of Nip1p.** *A,* growth of DG-452 in galactose medium and glucose medium. A culture was started in YP medium containing 0.5% galactose, 1.5% raffinose at A_{600} approximately 0.1. At zero time, when the cells had entered log phase, half of the culture was pelleted by centrifugation and resuspended in YP medium containing 2% glucose. A_{600} readings were made at the times indicated, and the cultures were diluted with the appropriate medium as necessary to keep the readings between 0.1 and 0.3. *Circles,* galactose medium. *Squares,* glucose medium. *B,* Nip1p content of wild-type and DG-452 cells grown in galactose and glucose medium. Wild-type Ad cells were grown in YPD glucose medium to A_{600} = 0.5. DG-452 cells were grown in YP medium containing 0.5% galactose, 1.5% raffinose to A_{600} = 0.5, then shifted to YPD medium for varying times. The A_{600} was maintained at 0.5 or less by diluting with fresh medium. Extracts were analyzed for the presence of Nip1p by immunoblotting with affinity purified antibody. The sizes in kilodaltons of prestained protein molecular mass markers are indicated on the *left*. The positions of full-length Nip1p (*Band A*) and its two major degradation products (*Bands B* and *C*) are indicated on the *right*. For the DG-452 cells, extract from equal amounts of cells on the basis of A_{600} was placed in each lane. For the Ad cells, half this amount of extract was used. *Lane 1,* Ad cells. *Lanes 2–7,* DG-452 cells incubated for 0, 2, 4, 6, 12.5, and 19 h in YPD medium.

Depleting Cells of Nip1p Affects General Protein Synthesis and Cell Growth—To investigate further the possible role of Nip1p in protein synthesis, we constructed strain DG-452 which could be depleted of Nip1p by glucose repression. To facilitate depletion, a ubiquitin-*NIP1* fusion gene was used that incorporated the destabilizing amino acid arginine at the Nip1p N terminus (23). Fig. 2*A* shows that the growth rate of this strain, estimated from A_{600} measurements, began to decrease about 10 h after transferring from medium containing galactose to medium containing glucose, whereas the growth rate of cells maintained in galactose medium did not diminish. Immunoblot analysis confirmed that cellular levels of Nip1p decreased following the shift to glucose medium. Fig. 2*B, lane 1,* shows that an extract from Ad wild-type cells grown in glucose medium contains a major band equivalent to the 93-kDa size predicted for full-length wild-type Nip1p (Band A) and a cross-reactive ~66 kDa (Band B) that we assume to be a degradation product. *Lanes 2–7* show extracts from the DG-452 strain grown in galactose medium (0 h in glucose medium), then incubated in glucose medium for 2, 4, 6, 12.5, and 19 h. In the DG-452 extract at zero time (*lane 2*), the major anti-Nip1p cross-reactive band was Band B (*lane 2*). Full-length ubiquitin-R-Nip1p (band A, *lane 2*) migrated slightly slower than native Nip1p (Band A, *lane 1*). Ubiquitin-R-Nip1p expressing cells contained an additional ~53-kDa degradation product (Band C, *lanes 2* and *3*). During incubation in glucose medium, the

fraction of ubiquitin-R-Nip1p in full-length protein appeared to increase while the total amount was decreasing (*lanes 3–7*). By 12.5 h, Nip1p was barely detectable (*lane 6*), and by 19 h, it was undetectable (*lane 7*). Densitometry of this blot revealed that the total amount of ubiquitin-R-Nip1p per cell, expressed as the sum of Bands A, B, and C, decreased with an apparent half-life of 3 h. After 12.5 h, less than 10% remained. During this period, the total protein content of the cells varied less than 2-fold (data not shown).

The stability of Nip1p and ubiquitin-R-Nip1p varied among strains. Full-length Nip1p was readily extracted from B-8106 cells without the use of protease inhibitors (Figs. 5–7), whereas protease inhibitors were required to isolate full-length Nip1p from Ad and DG-452 cells. As is apparent in Fig. 2*B*, ubiquitin-R-Nip1p was extremely labile in DG-452 cells even when protease inhibitors were used during preparation of the extracts.

Protein synthesis rates in wild-type and Nip1p-depleted cells were determined by measuring [^{35}S]methionine/cysteine incorporation in DG-452 after a shift from galactose to glucose medium. As shown in Fig. 3, the protein synthesis rate decreased immediately after shifting from galactose to glucose medium, and leveled off at ~15% of the zero time rate between 19 and 22 h. In other experiments, synthesis rates in DG-452 cells increased slightly between 0 and 2 h after the shift to glucose medium before declining to low levels (data not shown). In contrast, protein synthesis rates in Ad wild-type cells increased and remained higher following the shift to glucose medium (Fig. 3). We report elsewhere that cells depleted of Nip1p are deficient in cell-free translation, and that cell-free translation is restored by a purified protein complex containing Nip1p (42).

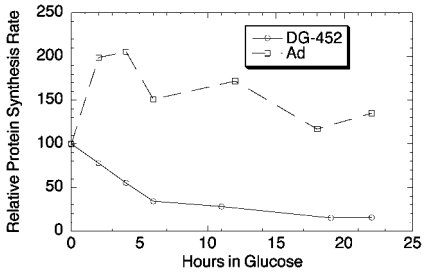

FIG. 3. **Protein synthesis rates in DG-452 cells and Ad wild-type cells grown in galactose medium (0 h in glucose medium), then shifted to glucose medium for the indicated times.** Protein synthesis rates were measured as described under "Materials and Methods." *Circles,* DG-452 cells. *Squares,* Ad wild-type cells.

Deficiency of Nip1p Affects Translation Initiation—Analysis of polysome profiles in sucrose density gradients is a sensitive method for detecting defects in translation initiation. A reduced initiation rate results in a decreases in polysome size and the fraction of ribosomes in polysomes and a concomittant increase in the fraction of ribosomes in monosomes and subunits. The potential role of Nip1p in translation initiation was investigated by analyzing polysome extracts from DG-452 cells depleted of Nip1p by incubating for various times in glucose medium. Fig. 4*A* shows that by 6 h in glucose medium, there was a reduction in polysome content accompanied by an increase in the amount of monosomes and ribosomal subunits. After 19 h of incubation in glucose medium, only about 10% of the total ribosomes were present in polysomes. An extract from Ad wild-type cells grown in glucose medium gave a polysome profile and polysome content very similar to DG-452 cells grown in galactose medium (data not shown). The relative amount of polysomes after shift of DG-452 cells to glucose medium is depicted graphically in Fig. 4*B*. The data from two independent experiments were very similar. The decrease in polysome content following shift to glucose medium and depletion of Nip1p shows that Nip1p is indeed required for transla-

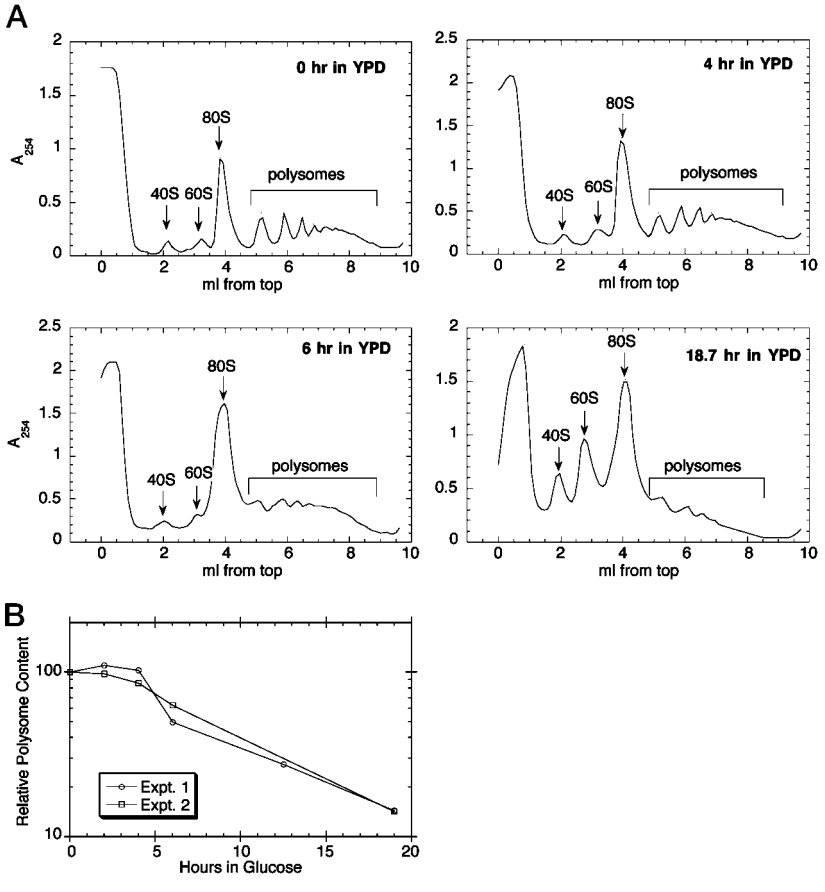

FIG. 4. **Cells depleted of Nip1p are defective in translation initiation.** *A,* sucrose gradient analysis of DG-452 extracts grown in galactose medium, then shifted to glucose medium for the indicated times. Extracts from equal amounts of cells were analyzed by sucrose density gradient centrifugation. Optical scans of the gradients are shown. *B,* decay of polysomes in DG-452 cells The sucrose gradient scans of *A* were analyzed by measuring the relative areas under the polysome, monosome, and ribosomal subunit peaks. The polysome content was expressed as the percent of total ribosomes in polysomes, then normalized to 100% at zero time. The *squares* and *circles* correspond to two independent experiments.

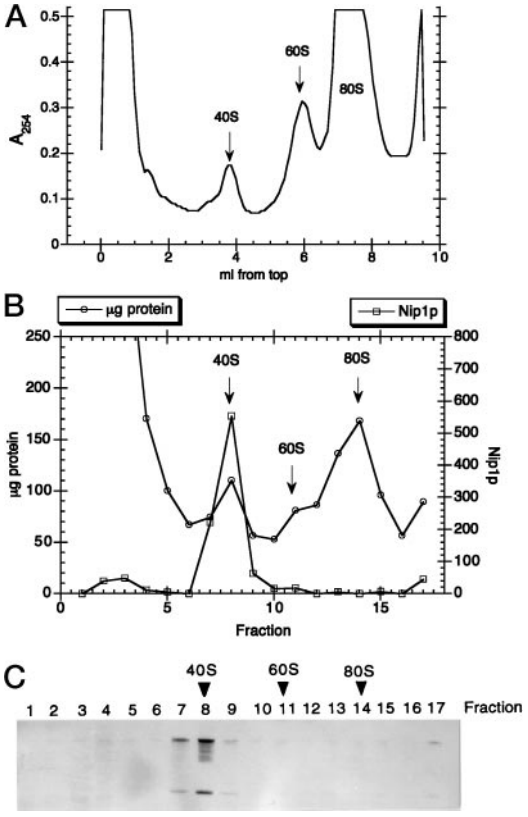

FIG. 5. **Cosedimentation of Nip1p with small ribosomal subunits.** NIP1$^+$ (B-8106) cells were grown to early log phase at 30 °C in YPD. Ribosomal subunits and ribosomes were separated on sucrose gradients for 6 h at 41,000 rpm in 15–30% sucrose gradients in the Beckman SW41 rotor. *A,* A_{254} scan of the gradient. *B,* distribution in the above sucrose density gradient of total protein estimated by the Bradford assay (67) (*open circles*) and Nip1p estimated by quantitative densitometry of an immunoblot (*open squares*). *C,* immunoblot used for densitometry. Only the relevant portion of the blot is shown. The *topmost band* corresponds to 93-kDa full-length Nip1p; the *lower band* is a degradation product of about 66 kDa. The relative amount of Nip1p in the fractions was quantified by scanning the blot with a HP ScanJet IIcx/T (Hewlett-Packard, Palo Alto) and analyzing the scans with NIH Image software.

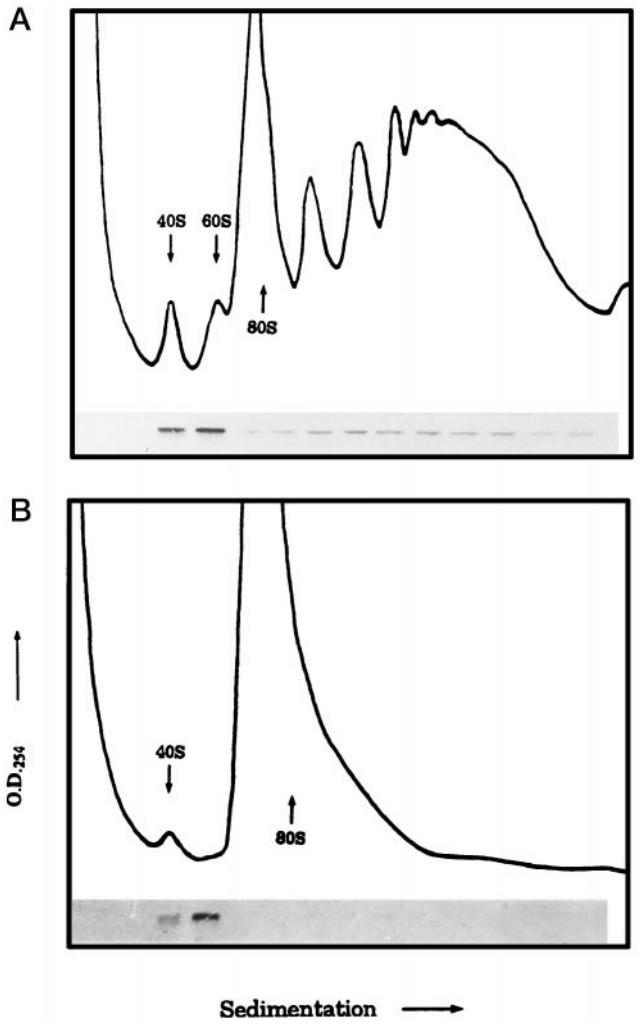

FIG. 6. **Nip1p in polysomes is associated with small ribosomal subunits.** NIP1$^+$ (B-8106) cells were grown to early log phase at 30 °C in YPD. The distribution of Nip1p in the gradient fractions was assayed by immunoblotting with anti-Nip1p antibody. Portions of the immunoblots are shown aligned with the optical scans of the gradients. *A,* ribosomal subunits and ribosomes were resolved in sucrose gradients for 2.5 h. *B,* the cell extract was treated with boiled 0.3 mg/ml RNase A for 30 min on ice prior to centrifugation.

tion initiation. The effect of growth at a nonpermissive temperature on the polysomes in *nip1-1* cells was also studied. *nip1-1* cells shifted to 37 °C for 4.5 h resulted in a 50% decrease in the fraction of ribosomes in polysomes compared with results to *nip1-1* cells grown at 30 °C (data not shown).

Nip1p Cosediments with 40 S Ribosomal Subunits—To investigate whether Nip1p associates with ribosomes, cell extracts from strain B-8106 (*NIP1*$^+$) were separated on a sucrose gradient and probed by immunoblotting with polyclonal anti-Nip1p antiserum. Fig. 5*A* shows the distribution of 40 S, 60 S, and 80 S ribosomes across the gradient. Fig. 5*B* shows the distribution of total protein and Nip1p in the gradient fractions. The distribution of Nip1p was estimated by quantitative densitometry of the immunoblot shown in Fig. 5*C*. The total protein distribution shows peaks corresponding to 40 S, 60 S, and 80 S ribosomes. The bulk of Nip1p cosedimented with 40 S subunits. A small amount of Nip1p sedimented at the top of the gradient, but only traces were associated with 60 S or 80 S ribosomes. In Fig. 5, polysomes were sedimented to the bottom of the gradient. Fig. 6*A* shows the distribution of Nip1p across a gradient that displayed polysomes. Here it is apparent that Nip1p associates both with 40 S subunits and with polysomes.

The observation that Nip1p is associated primarily with 40 S ribosomal subunits and polysomes, but not with 80 S subunits or monosomes, suggested that the polysomal Nip1p might be in the form of 48 S preinitiation complexes bound to mRNA and not, for instance, in association with translating 80 S ribosomes. To test this hypothesis, we treated extracts with RNase. After RNase treatment, any Nip1p associated with 80 S ribosomes would sediment at the position of 80 S monosomes. Fig. 6*B* shows that after RNase treatment, Nip1p sedimented exclusively in the 40–48 S region of the sucrose gradient. The 60 S subunit peak was not visible in this gradient, presumably because it was not resolved from the very large monosome peak. It is therefore likely that polysomal Nip1p is associated with 48 S preinitiation complexes.

Nip1p Cosediments with Halfmers—To investigate further the association of Nip1p with 40 S ribosomes, we examined the distribution of Nip1p across a polysome gradient prepared from a strain that produces significant amounts of halfmer polysomes. Halfmers occur when 40 S preinitiation complexes accumulate on mRNAs, when, for example, cells become depleted of 60 S subunits. Halfmers appear as shoulders or discrete peaks that contain one, two, or three 80 S ribosomes and an additional 40 S preinitiation complex. In one such halfmer-producing strain, Foiani *et al*. (43) showed that the 80 S halfmer shoulder was enriched in 18 S rRNA to an extent that

was consistent with an extra 48 S preinitiation complex. If Nip1p is associated with 48 S preinitiation complexes and not with elongating 80 S ribosomes, then it too should be concentrated in the halfmer shoulders. When an immunoblot of of polysome gradient fractions from the halfmer-producing strain DG-130 (44) was probed with antibody against Nip1p, Nip1p was indeed found to be enriched in the halmer shoulders (data not shown). This experiment confirmed the conclusion from the RNase experiment of Fig. 6 that Nip1p associated with polysomes is present in 40 S preinitiation complexes.

Nip1p Is a Subunit of a High Molecular Weight Complex Containing Translation Initiation Factor Prt1p—The results described above suggest that Nip1p is involved in the initiation step of protein synthesis. Further support for this conclusion comes from the fact that one of the subunits of human translation initiation factor 3 (eIF3) is 31% identical to yeast Nip1p (2). To determine if Nip1p is present in eIF3, we tagged the C terminus of Prt1p with a stretch of eight histidines (Prt1p-His) and employed Ni^{2+} affinity chromatography to isolate proteins associated with this tagged form of Prt1p, referred to as Prt1p-His. An extract from cells expressing untagged Prt1p was used as a control. We first evaluated whether the His-tag affected the function of Prt1p *in vivo* by determining whether the His-*PRT1* allele could complement the lethal phenotype of a *prt1*Δ allele. *His-PRT1* was introduced on a single copy plasmid into a *prt1*Δ strain by plasmid shuffling (see "Materials and Methods"). The resulting strain, LPY201, had a growth rate indistinguishable from the isogenic *prt1*Δ strain containing wild-type *PRT1* on a plasmid (data not shown). We conclude that the His-tag did not significantly affect Prt1p function.

To determine whether Nip1p is associated with Prt1p, we prepared RSW fractions, which are enriched for initiation factors, from strains expressing tagged Prt1p-His (LPY201) or untagged Prt1p (LPY200) and incubated both preparations with Ni^{2+}-NTA-agarose resin. The eluate fractions were resolved by SDS-PAGE and analyzed by immunoblotting using polyclonal antibodies against Prt1p and Nip1p. Fig. 7*A* shows that both Prt1p-His and Nip1p specifically bound to and eluted from the Ni^{2+}-NTA resin in a manner that was completely dependent on His-tagged Prtp1p. These results support the hypothesis that Nip1p is specifically associated with Prt1p in the RSW fraction.

Because Prt1p has been shown to reside in heteromeric complexes larger than 300 kDa (6, 16), we next sought to demonstrate that Nip1p and Prt1p copurify in the same high molecular mass complex. To accomplish this, whole cell extracts were prepared from strains LPY100 and LPY101 and purified on Ni^{2+}-NTA-agarose. The resulting eluates were then separated by size using gel filtration chromatography. Analysis of the resulting fractions from the *PRT1-His* strain by SDS-PAGE and silver staining revealed five major polypeptides with apparent masses of 110, 93, 90, 39, and 32 kDa coeluting in fractions 36–39 (Fig. 7*B*), with the peak fraction (number 38) corresponding to a molecular mass of 600–670 kDa. Immunoblot analysis showed the major 93- and 90-kDa polypeptides in fractions 36–39 corresponded to Nip1p and Prt1p, respectively. This conclusion was based on the fact that the corresponding immunoreactive and silver-stained bands migrated identically in SDS-PAGE and are distributed similarly throughout the column fractions (Fig. 7*B*). None of the five major polypeptides visible by silver staining were detected in the corresponding column fractions obtained using a preparation from the untagged *PRT1* strain (data not shown); thus, the 110-, 39-, and 32-kDa polypeptides, as well as Nip1p, are specifically associated with Prt1p in a high molecular mass complex. The results in Fig. 7*B* were obtained using strains containing the chromosomal *prt1-1* mutant allele. Virtually identical results have been obtained using RSW fractions from LPY200 and LPY201, described above, in which chromosomal *PRT1* is deleted. The relative masses of Prt1p, Nip1p, and the three other major polypeptides shown to be associated with Prt1p-His in Fig. 7*B* are similar to those of the 5-subunit complex containing Prt1p, isolated by Danaie *et al.* (16), which restored translation to a *prt1-1* mutant extract. We show elsewhere that the 110-kDa subunit corresponds to gene product YBR079C which is the yeast homolog of human eIF3-p170 (42). Similarly, the 39- and 32-kDa subunits, respectively, correspond to the Tif34p subunit of yeast eIF3 and the YDR429c (p33) gene product which is the yeast homolog of human eIF3-p44 (42).

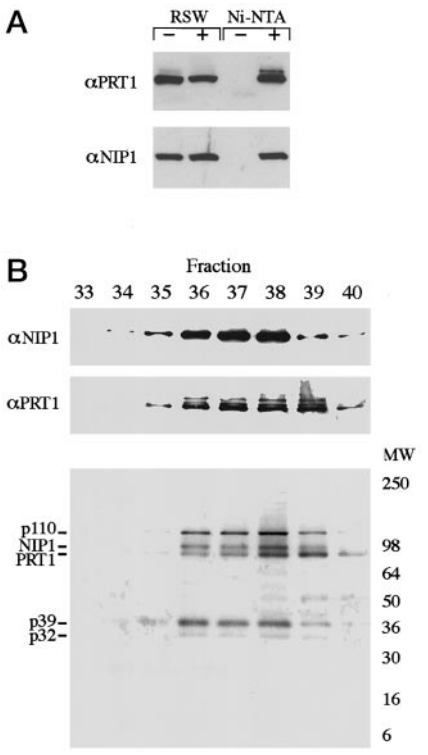

FIG. 7. **Biochemical evidence that Nip1p is a component of a high molecular weight complex containing Prt1p.** *A*, specific interaction between Nip1p and His-tagged Prt1p in the RSW fraction. RSW fractions prepared in parallel from strain LPY200 expressing untagged Prt1p (−) and LPY201 expressing Prt1p-His (+) were purified on Ni^{2+}-NTA-agarose. About 25 μg of RSW and 0.5 μg of the eluate from Ni^{2+}-NTA-agarose was separated by 4–20% gradient SDS-PAGE, transferred to nitrocellulose, and probed with antibodies against Prt1p (αPRT1) at 1:1,000 dilution, or against Nip1p (αNIP1) at 1:1,000 dilution. The immune complexes were visualized using alkaline phosphatase-conjugated antibodies (1:5000 dilution) against rabbit IgG and the enhanced chemiluminescence kit purchased from Amersham. *B,* Nip1p and Prt1p reside in the same high molecular weight complex. Whole cell extract prepared from strain LPY101 was purified on Ni^{2+}-NTA-agarose and then size-fractionated by fast protein liquid chromatography on a Sepharose-6 column. Aliquots (25 μl) of fractions from the Sepharose-6 column were separated by 4–20% gradient SDS-PAGE and analyzed by immunoblot analysis (*top panel*) using antibodies against Prt1p (αPRT1) or Nip1p (αNIP1), or by silver staining (*bottom panel*). The fraction numbers (33–40) are listed above the blot with fraction 38 corresponding to the elution volume of thyroglobulin, a 670-kDa protein standard from Bio-Rad. The migration positions of Nip1p (about 95 kDa), Prt1p (about 90 kDa), p110, p39, and p32 are indicated on the *left* of the *bottom panel*. The migration positions of molecular weight (MW) markers are shown on the *right*.

Cells Depleted of Nip1p Are Not Depleted of Nip1p-associated Proteins—When cells are depleted of the Tif34p subunit of eIF3, other subunits of eIF3 are rapidly degraded (9). To find out if Nip1p-associated proteins are degraded when cells are depleted of Nip1p, extracts from DG-452 cells depleted of Nip1p

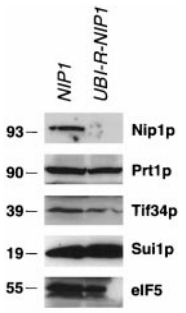

FIG. 8. **Cells depleted of Nip1p are not depleted of Nip1p-associated proteins.** Whole cell extracts prepared from isogenic strains DG-452 (*UBI-R-NIP1*) (incubated in glucose medium for 17 h) and Ad (*NIP1*) (grown in glucose medium) were analyzed by immunoblotting with antibodies against the proteins listed on the *right* of each panel. Equal amounts of total protein (50 μg) from each strain were resolved by 4–20% gradient SDS-PAGE and subjected to analysis using the following primary antibodies diluted in TBST (25 mM Tris-HCl, pH 7.4, 14 mM NaCl, 2.7 mM KCl, 0.01% Tween 20, and 5% non-fat milk): affinity purified anti-Nip1p (1:200), anti Prt1p (1:1,000), anti-eIF5 (1:2, 500), anti-Tif34p (1:500), and anti-Sui1p (1:1,000). Immunodetection was performed using horseradish peroxidase-conjugated anti-rabbit second antibody and developed using a chemiluminescence kit (ECL 228) from Amersham.

by incubation in glucose medium were probed with antibodies to other proteins in the Prt1p-His complex. Fig. 8 shows that, even though Nip1p was depleted to undetectable levels, there was no change in the amounts of Prt1p or Tif34p. We show elsewhere that the Sui1p subunit of yeast eIF3 and also, initiation factor eIF5, are specifically associated with Prt1p-His when whole cell extracts made in low salt are chromatographed on the Ni^{2+}-NTA column (42). The levels of the latter two proteins are also unchanged when cells are depleted of Nip1p (Fig. 8).

DISCUSSION

Involvement of Nip1p in Translation—Several lines of evidence indicate that Nip1p plays a role in the initiation of protein synthesis as a conserved subunit of eIF3. 1) The overall rate of protein synthesis is reduced in cells depleted of Nip1p; the reduction in the protein synthesis rate occurs before the growth rate is affected. 2) Cells depleted of Nip1p are defective in translation initiation as judged from polysome profiles. 3) Nip1p is associated with 40 S ribosomal subunits in preinitiation complexes and polysomes. 4) Cell extracts depleted of Nip1p are defective in *in vitro* translation initiation. 5) Nip1p occurs in a complex with Prt1p, a known component of translation initiation factor eIF3 (6). Other results are also consistent with a role for Nip1p in translation initiation. 1) Deletion of the *RPL46* gene suppresses the temperature sensitivity of growth in the *nip1-1* mutant. Mutations in *RPL46* were previously shown to suppress mutations of *PAB1* (36) and *SIS1* (37), both of which have been implicated in translation initiation. 2) *nip1-1* cells are hypersensitive to paromomycin.

Suppression of nip1-1 Mutant by Mutation or Deletion of RPL46—The observation that deletion or mutation of *RPL46*, which codes for a 60 S subunit protein, suppresses the *nip1-1* ts growth defect seems paradoxical in view of the association of Nip1p with 40 S subunits. It is possible that Nip1p and the 60 S subunit interact transiently, for example, during the 40–60 S joining step, when *RPL*46 deletion could have a direct effect on initiation. Indeed, we show elsewhere that there is direct interaction between Nip1p and eIF5 on the basis of two-hybrid and *in vitro* binding studies (42). eIF5 is a GTP-hydrolyzing initiation factor required for the 40–60 S joining step, which causes release of eIF2-GDP and eIF3 from the 40 S ribosomal subunit (45–49). It is assumed here that deletion or mutation of *RPL46* suppresses the *nip1-1* mutation by altering the structure/function of the 60 S subunit. However, it has not been ruled out that suppression is a kinetic effect due to the reduced concentration of 60 S subunits in cells deficient in *RPL46* function (36).

Paromomycin Sensitivity of nip1-1 Mutant—The aminoglycoside antibiotic paromomycin is thought to cause translational misreading by binding to the decoding site of the small ribosomal subunit (50, 51). Paromomycin sensitivity has previously been found in yeast strains having suppressor mutations which by themselves cause translational misreading (52). Two of the suppressor genes, *SUP35* and *SUP45*, code for termination factors (53–55). *SUP44* codes for a small subunit ribosomal protein (56). As far as we know, paromomycin sensitivity has not been reported previously for mutant initiation factors. However, it seems plausible that paromomycin could affect the function of any protein involved in the decoding process. Some initiation factors are known to be involved in translation start site selection, and therefore, must be involved in decoding. These include Sui2p and Sui3p which are subunits of eIF2 (57, 58). They also include Sui1p/p16 which is a subunit of eIF3 (8) and eIF5 (59). The paromomycin sensitivity of the *nip1-1* mutant suggests that Nip1p might also be involved in translation start site selection, and conversely, that mutants of other initiation factors involved in translation start site selection may have altered paromomycin sensitivity. Interestingly, Nip1p interacts with Sui1p as well as eIF5 (60). These observations, taken together with suppression of *nip1-1* by deletion of *RPL46*, suggest that Nip1p, Sui1p, and eIF5 function as a complex in translation start site selection and the 40–60 S joining step.

Cells Depleted of Nip1p Have a Reduced Rate of Protein Synthesis and Are Defective in Translation Initiation—The amount of Nip1p began to decrease immediately after shifting DG-452 cells from galactose medium to glucose medium. In one experiment, the protein synthesis rate also began to decrease immediately upon shift to glucose medium. In other experiments, the protein synthesis rate began to decrease after a lag of about 2 h. The polysome content began to decrease after a lag of 2–4 h in two experiments. The observation that the protein synthesis rate began to decrease before there was a perceptible decrease in the cell growth rate argues that the decrease in protein synthesis causes the decrease in growth rate, rather than *vice versa*. This conclusion is supported by the reversible translation defect in extracts from cells depleted of Nip1p (42). Whether or not there is a lag before the protein synthesis rate and polysome content begin to decrease following shift to glucose medium would depend on whether or not the initial level of Nip1p is rate-limiting for protein synthesis. Cells were grown in 0.5% galactose, 1.5% raffinose, rather than 2% galactose, to avoid overexpressing Nip1p.

To facilitate the decay of Nip1p following shift to glucose medium, wild-type Nip1p was replaced by a ubiquitin-Nip1p fusion protein in which the Nip1p coding sequence began with the destabilizing amino acid, arginine. The content per cell of the fusion protein decreased with an apparent half-life of about 3 h, which is similar to the 2–3 h initial doubling time of the cells and suggests that the protein is fairly stable. Nevertheless, the use of this construct was crucial to the success of the experiments. A ubiquitin-Nip1p fusion construct was also made in which the Nip1p coding sequence started with the stabilizing amino acid, methionine. However, the strain which had the M protein in place of the R protein, DG-455, grew normally in glucose medium, presumably because of the in-

creased stability of the protein.[2]

Depletion of a putative translation initiation factor by means of glucose repression of a *GAL* promoter has previously been utilized to investigate the function of the factor. In the case of Tif34p, which is thought to be a component of yeast eIF3, depletion resulted in a decrease in polysome content similar to the results obtained for Nip1p (9). In contrast, depletion of the hypusine-containing factor eIF5A halted cell growth with minimal effects on protein synthesis and polysome content (61). It was concluded that eIF5A is not required for general protein synthesis (61).

Is Nip1p a Subunit of eIF3?—The facts that Nip1p functions in translation initiation and copurifies in a large complex with *bona fide* subunits of eIF3, indicate that Nip1p is, in fact, a subunit of eIF3. Also, the putative human homologue of Nip1p co-purified with human eIF3 (2). However, this question cannot be answered unequivocally because of uncertainty about the nature of eIF3. Including ours, three different presumptive eIF3 complexes containing Prt1p have been purified from yeast. The 5-subunit complex isolated by Danaie *et al.* (16) complemented a *prt1-1* cell-free extract for reduced incorporation of methionine into 40 S preinitiation complexes, and thus appears to possess an activity ascribed to mammalian eIF3. This complex is highly similar in subunit composition and molecular weight to that purified here by Ni^{2+}-affinity chromatography from a strain containing a His-tagged form of Prt1p. We concluded that Nip1p is the second largest subunit of this complex because it reacted specifically with antibodies raised against a Nip1p fusion protein expressed in bacteria and because its apparent mass is close to that predicted for Nip1p. To confirm the antibody identification, we have also used mass spectrometry to show that Nip1p and Prt1p are the second and third largest subunits, respectively, of the complex we purified (42). In addition, we found that the 39-kDa subunit of our complex is identical to the p39 subunit of the eIF3 complex isolated by Naranda *et al.* (6). The latter was purified by its ability to functionally substitute for human eIF3 in an *in vitro* assay for translation initiation (6). The complex isolated by Naranda *et al.* (6) and that described here both contained a 32–33-kDa subunit now called Tif35p (12). Thus, the complex we identified containing Nip1p also contains three other proteins identified previously as subunits of yeast eIF3. In addition, Prt1p, Nip1p, and p39 are homologous to the p116, p110 and p36 subunits, respectively, of human eIF3 (2). Based on these findings, we suggest that the 5-subunit complex described here encompasses the core constituents of yeast eIF3. This conclusion is in accordance with our observation that Nip1p binds to free and polysome-associated 40 S subunits since, in mammalian cells, eIF3 is a stable constituent of 43 S preinitiation complexes (1). The fact that Nip1p depletion leads to a defect in translation initiation *in vivo* and *in vitro* suggests that Nip1p is required for a critical function of eIF3 in translation initiation.

A difference between our complex and that of Naranda *et al.* (6) is that intact Nip1p and the 110-kDa polypeptide (YBR079c) present in our complex were not detected by Naranda *et al.* This could indicate that Nip1p and p110 are dispensable for stimulating methionyl-puromycin synthesis; alternatively, the preparations of Naranda *et al.* (6) may have contained degradation products of these proteins which supplied functions required for the reaction. Another difference is that the eIF3 complex isolated by Naranda *et al.* (6) contained Gcd10p (the 62-kDa subunit) (10) and Sui1p (the 16 kDa subunit) (8). Perhaps these proteins are not integral subunits of eIF3 but copurified with it because they promote its ability to stimulate methionyl-puromycin synthesis.

Another possibility is that the complex isolated by Naranda *et al.* (6) represents a different functional form of eIF3 from the one isolated by ourselves and by Danaie *et al.* In addition to uncertainty about the composition of eIF3, little is known about the functions of individual subunits. It is not known if they have any function by themselves, or if they function only in concert with some or all of the other subunits. Also, it is not known if the complex is metabolically static, or if interactions between the subunits are dynamic.

Relationship between Nuclear Transport and Protein Synthesis Defects of the nip1-1 Mutant—Although the *nip1-1* mutant was isolated in a screen for nuclear import mutants and is defective in nuclear import, the relationship between the mutation and the defect is not known. One possibility is that Nip1p is a dual function protein with separate roles in protein synthesis and nuclear import. Some other translation factors are known to have multiple functions (62–66). Finally, we cannot rule out that protein synthesis and nuclear transport are coupled in yeast, and that a defect in protein synthesis translates to a defect in nuclear transport.

Acknowledgments—We thank T. Naranda, J. Hershey, and N. Sonenberg for sharing results prior to publication and Nilson Zanchin for helpful discussions.

[2] J. R. Greenberg, unpublished observations.

REFERENCES

1. Merrick, W. C., and Hershey, J. W. B. (1996) in *Translational Control* (Hershey, J. W. B., Matthews, M. B., and Sonenberg, N., eds) pp. 31–69, Cold Spring Harbor Laboratory, Cold Spring Harbor, NY
2. Asano, K., Kinzy, T. G., Merrick, W. C., and Hershey, J. W. B. (1997) *J. Biol. Chem.* **272,** 1101–1109
3. Asano, K., Merrick, W. C., and Hershey, J. W. B. (1997) *J. Biol. Chem.* **272,** 23477–23480
4. Asano, K., Vornlocher, H.-P., Richter-Cook, N. J., Merrick, W. C., Hinnebusch, A. G., and Hershey, J. W. B. (1997) *J. Biol. Chem.* **272,** 27042–27052
5. Methot, N., Rom, E., Olsen, H., and Sonenberg, N. (1997) *J. Biol. Chem.* **272,** 1110–1116
6. Naranda, T., MacMillan, S. E., and Hershey, J. W. B. (1994) *J. Biol. Chem.* **269,** 32286–32292
7. Yoon, H., and Donahue, T. F. (1992) *Mol. Cell. Biol.* **12,** 248–260
8. Naranda, T., MacMillan, S. E., Donahue, T. F., and Hershey, J. W. B. (1996) *Mol. Cell. Biol.* **16,** 2307–2313
9. Naranda, T., Kainuma, M., MacMillan, S. E., and Hershey, J. W. B. (1997) *Mol. Cell. Biol.* **17,** 145–153
10. Garcia-Barrio, M. T., Naranda, T., Vazquez de Aldana, C. R., Cuesta, R., Hinnebusch, A. G., Hershey, J. W. B., and Tamame, M. (1995) *Genes Dev.* **9,** 1781–1796
11. Hanic-Joyce, P. J., Singer, R. A., and Johnston, G. C. (1987) *J. Biol. Chem.* **262,** 2845–2851
12. Verlhac, M. H., Chen, R. H., Hanachi, P., Hershey, J. W. B., and Derynck, R. (1997) *EMBO J.* **16,** 6812–6822
13. Hershey, J. W. B., Asano, K., Naranda, T., Vornlocher, H.-P., and Hanachi, P. (1996) in *Post-transcriptional Control of Gene Expression: The Regulatory Role of RNA,* International OJI Seminar, Hakone, Japan
14. Kasperaitis, M. A., Voorma, H. O., and Thomas, A. A. (1995) *FEBS Lett.* **365,** 47–50
15. Dever, T. E., Yang, W., Astrom, S., Bystrom, A. S., and Hinnebusch, A. G. (1995) *Mol. Cell. Biol.* **15,** 6351–6363
16. Danaie, P., Wittmer, B., Altmann, M., and Trachsel, H. (1995) *J. Biol. Chem.* **270,** 4288–4292
17. Gu, Z., Moerschell, R. P., Sherman, F., and Goldfarb, D. S. (1992) *Proc. Natl. Acad. Sci. U. S. A.* **89,** 10355–10359
18. Gu, Z. (1995) *Studies of Nuclear Transport and Function of NIP1 in the Yeast Saccharomyces cerevisiae.* Ph.D. Thesis, University of Rochester, Rochester, NY
19. Rose, M. D., Novick, P., Thomas, J. H., Botstein, D., and Fink, G. R. (1987) *Gene* (*Amst.*) **60,** 237–243
20. Gietz, R. D., and Sugino, A. (1988) *Gene* (*Amst.*) **74,** 527–534
21. Sherman, F., Fink, G. R., and Hicks, J. B. (1987) *Methods in Yeast Genetics*, Cold Spring Harbor Laboratory, Cold Spring Harbor, NY
22. Sherman, F. (1991) *Methods Enzymol.* **194,** 3–21
23. Park, E.-C., Finley, D., and Szostak, J. W. (1992) *Proc. Natl. Acad. Sci. U. S. A.* **89,** 1249–1252
24. Sikorski, R. S., and Hieter, P. (1989) *Genetics* **122,** 19–27
25. Yon, J., and Fried, M. (1989) *Nucleic Acids Res.* **17,** 4895
26. Iizuka, N., Najita, L., Franzusoff, A., and Sarnow, P. (1994) *Mol. Cell. Biol.* **14,** 7322–7330
27. Güldener, U., Heck, S., Fielder, T., Beinhauer, J., and Hegemann, J. H. (1996) *Nucleic Acids Res.* **24,** 2519–2524
28. Gietz, D., St. Jean, A., Woods, R. A., and Schiestl, R. H. (1992) *Nucleic Acids Res.* **20,** 1425
29. Boeke, J. D., Lacroute, F., and Fink, G. R. (1984) *Mol. Gen. Genet.* **197,**

345–346
30. Wach, A., Brachat, A., Pohlmann, R., and Philippsen, P. (1994) *Yeast* **10,** 1793–1808
31. Ito, H., Fukuda, Y., Murata, K., and Kimura, A. (1983) *J. Bacteriol.* **153,** 163–168
32. Devereux, J. P., Haeberli, P., and Smithies, O. (1984) *Nucleic Acids Res.* **12,** 387–395
33. Cigan, A. M., Foiani, M., Hannig, E. M., and Hinnebusch, A. G. (1991) *Mol. Cell. Biol.* **11,** 3217–3228
34. Leer, R. J., van Raamsdonk-Duin, M. M., Kraakman, P., Mager, W. H., and Planta, R. J. (1985) *Nucleic Acids Res.* **13,** 701–709
35. Sachs, A. B., and Davis, R. W. (1990) *Science* **247,** 1077–1079
36. Sachs, A. B., and Davis, R. W. (1989) *Cell* **58,** 857–867
37. Zhong, T., and Arndt, K. T. (1993) *Cell* **73,** 1175–1186
38. Lee, W.-C., and Mélèse, T. (1989) *Proc. Natl. Acad. Sci. U. S. A.* **86,** 8808–8812
39. Lee, W.-C., Xue, Z. X., and Mélèse, T. (1991) *J. Cell Biol.* **113,** 1–12
40. Palmer, E., Wilhelm, J. M., and Sherman, F. (1979) *Nature* **277,** 148–150
41. Gale, E. F., Cundliffe, E., Reynolds, P. E., Richmond, M. H., and Waring, M. J. (1981) *The Molecular Basis of Antibiotic Action*, John Wiley and Sons, London
42. Phan, L., Zhang, X., Asano, K., Anderson, J., Vornlocher, H.-P., Greenberg, J. R., Qin, J., and Hinnebusch, A. G. (1998) *Mol. Cell. Biol.* **18**, in press
43. Foiani, M., Cigan, A. M., Paddon, C. J., Harashima, S., and Hinnebusch, A. G. (1991) *Mol. Cell. Biol.* **11,** 3203–3216
44. Zanchin, N. I. T., Roberts, P., DeSilva, A., Sherman, F., and Goldfarb, D. S. (1997) *Mol. Cell. Biol.* **17,** 5001–5015
45. Trachsel, H., and Staehelin, T. (1978) *Proc. Natl. Acad. Sci. U. S. A.* **75,** 204–208
46. Benne, R., and Hershey, J. W. B. (1978) *J. Biol. Chem.* **253,** 3078–3087
47. Peterson, D. T., Safer, B., and Merrick, W. C. (1979) *J. Biol. Chem.* **254,** 7730–7735
48. Raychaudhuri, P., Chaudhuri, A., and Maitra, U. (1985) *J. Biol. Chem.* **260,** 2140–2145
49. Chakrabarti, A., and Maitra, U. (1991) *J. Biol. Chem.* **266,** 14039–14045
50. Chernoff, Y. O., Vincent, A., and Liebman, S. W. (1994) *EMBO J.* **13,** 906–913
51. Purohit, P., and Stern, S. (1994) *Nature* **370,** 659–662
52. Wakem, L. P., and Sherman, F. (1990) *Genetics* **124,** 515–522
53. Frolova, L., Le Goff, X., Rasmussen, H. H., Cheperegin, S., Drugeon, G., Kress, M., Arman, I., Haenni, A.-L., Celis, J. E., Philippe, M., Justesen, J., and Kisselev, L. (1994) *Nature* **372,** 701–703
54. Zhouravleva, G., Frolova, L., Le Goff, X., Le Guellec, R., Inge-Vechtomov, S. G., Kisselev, L., and Philippe, M. (1995) *EMBO J.* **14,** 4065–4072
55. Stansfield, I., Jones, K. M., Kushnirov, V. V., Dagkesamanskaya, A. R., Poznyakovski, A. I., Paushkin, S. V., Nierras, C. R., Cox, B. S., Ter-Avanesyan, M. D., and Tuite, M. F. (1995) *EMBO J.* **14,** 4365–4373
56. All-Robyn, J. A., Brown, N., Otaka, E., and Liebman, S. W. (1990) *Mol. Cell. Biol.* **10,** 6544–6553
57. Donahue, T. F., Cigan, A. M., Pabich, E. K., and Valavicius, B. C. (1988) *Cell* **54,** 621–632
58. Cigan, A. M., Pabich, E. K., Feng, L., and Donahue, T. F. (1989) *Proc. Natl. Acad. Sci. U. S. A.* **86,** 2784–2788
59. Huang, H. K., Yoon, H., Hannig, E. M., and Donahue, T. F. (1997) *Genes Dev.* **11,** 2396–2413
60. Asano, K., Phan, L., Anderson, J., and Hinnebusch, A. G. (1997) *J. Biol. Chem.* **273,** 18573–18585
61. Kang, H. A., and Hershey, J. W. B. (1994) *J. Biol. Chem.* **269,** 3934–3940
62. Yoon, H., Miller, S. P., Pabich, E. K., and Donahue, T. F. (1992) *Genes Dev.* **6,** 2463–2477
63. Gulyas, K. D., and Donahue, T. F. (1992) *Cell* **69,** 1031–1042
64. Jackson, R. J., Hunt, S. L., Gibbs, C. L., and Kaminski, A. (1994) *Mol. Biol. Rep.* **19,** 147–159
65. Yang, F., Demma, M., Warren, V., Dharmawardhane, S., and Condeelis, J. (1990) *Nature* **347,** 494–496
66. Shiina, N., Gotoh, Y., Kubomura, N., Iwamatsu, A., and Nishida, E. (1994) *Science* **266,** 282–285
67. Bradford, M. M. (1976) *Anal. Biochem.* **72,** 248–254